Biodesign

pISSN 2288-6982 | eISSN 2288-7105

CRYSTALLIZATION P 42-45

Purification and preliminary analysis of the regulatory domain of MexT from *Pseudomonas aeruginosa*, a LysR-type transcriptional activator of the MexEF-OprN multidrug efflux pump

Suhyeon Kim[1], Jinsook Ahn and Nam-Chul Ha[1]*

[1]Research Institute for Agriculture and Life Sciences, Center for Food and Bioconvergence, Center for Food Safety and Toxicology, Seoul National University, Seoul 08826, Republic of Korea

*Correspondence: hanc210@snu.ac.kr

Pseudomonas aeruginosa is an opportunistic pathogen, and have multiple multidrug efflux pumps. The MexEF-OprN multidrug efflux system is overexpressed in *nfxC*-type mutants and give resistance to quinolones, chloramphenicol and trimethoprim. A LysR-type transcriptional activator, MexT, is the major activator of this efflux system. Although the activity of MexT is regulated in response to the cellular redox state, the ligand and activation mechanism remain unknown yet. MexT consists of the N-terminal DNA binding domain and the C-terminal regulatory domain that contains the ligand binding site. In this study, we overproduced and purified the regulatory domain of MexT from *P. aeruginosa* and obtained the crystals suitable for the structural study. The crystal diffracted X-ray to 2.3 Å resolution, revealing that the crystals belong to space group $P2_12_12_1$, with unit cell parameters a = 65.7, b = 108.5, and c = 109.1 Å. The cell content analysis suggested that 3 or 4 molecules are contained in the asymmetric unit. To solve the phasing problem, growing of the Se-Met substituted crystals are underway. This structure will give insight into the molecular mechanism of the activation of MexT in the presence of antibiotics.

INTRODUCTION

The opportunistic pathogen *Pseudomonas aeruginosa* has a major clinical importance, and can rapidly develop resistance to diverse antibiotics that are structurally unrelated (Li et al., 2015). The bacteria are equipped with several efflux pumps in the resistance-nodulation-cell division (RND) family, whose structural assemblies were well characterized structurally (Jeong et al., 2016; Kim et al., 2015; Kohler et al., 1997; Song et al., 2015). Of these, the MexEF-OprN pump can exudate antibiotics, such as ciprofloxacin, chloramphenicol and trimethoprim. The expression of this efflux pump is normally shut down in wild type strain, but it is expressed at high levels in *nfxC*-type mutants, conferring the resistance to the pump substrate antibiotics (Kohler et al., 1997). Since the efflux pump is in chromosomally encoded, it is more challenging to treat the infection (Kohler et al., 1999).

MexT is located upstream of the *mexEF-oprN* operon, and was revealed as a positive regulator (Kohler et al., 1999; Kohler et al., 1997). MexT belongs to the LysR-type transcriptional regulator, which typically exhibit a characteristic tetrameric arrangement like the peroxide sensor OxyR (Jo et al., 2015) with some exceptions (Jang et al., 2018). LysR-type transcriptional regulators consist of a DNA binding domain in the N-terminal region, and a regulatory domain (RD) in the C-terminal region. Binding of the cognate ligand to the RD induces global conformational changes in their oligomeric assembly, leading to shifting DNA binding properties. It was reported that constitutive activation of MexT by miss-sense mutations resulted in high level expression of the MexEF-OprN in clinical isolates of *P. aeruginosa* (Juarez et al., 2018). However, it remains unknown how the mutation induced the constitutive activation of MexT. MexT is also involved in modulation of the global virulence of the bacteria, independent of the MexEF-OprN pump (Tian et al., 2009). It has been implicated that the predicted oxidoreductase MexS modulates the activation state of MexT by altering the redox state of cysteine residues in the RD (Fargier et al., 2012). It is still unknown which molecules trigger the activation of MexT. Thus, high resolution structures of MexT could be helpful to understand the molecular activation mechanism and the direct or indirect ligands for MexT, which may be essential to understand the antibiotic resistance. Herein, we report the overexpression and crystallization of the RD of MexT from *P. aeruginosa*, which would give insight into the molecular mechanism of the activation of MexT in the presence of antibiotics.

RESULTS AND DISCUSSION

We initially attempted to gain the full-length MexT from *P. aeruginosa* in the E. coli expression system. However, most

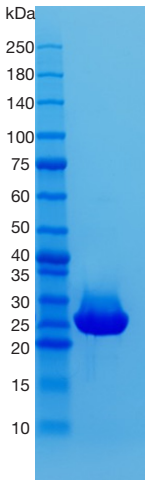

FIGURE 1 | The protein band on 4%-20% gradient SDS-polyacrylamide gel. The size marker proteins are presented in the left line (kDa).

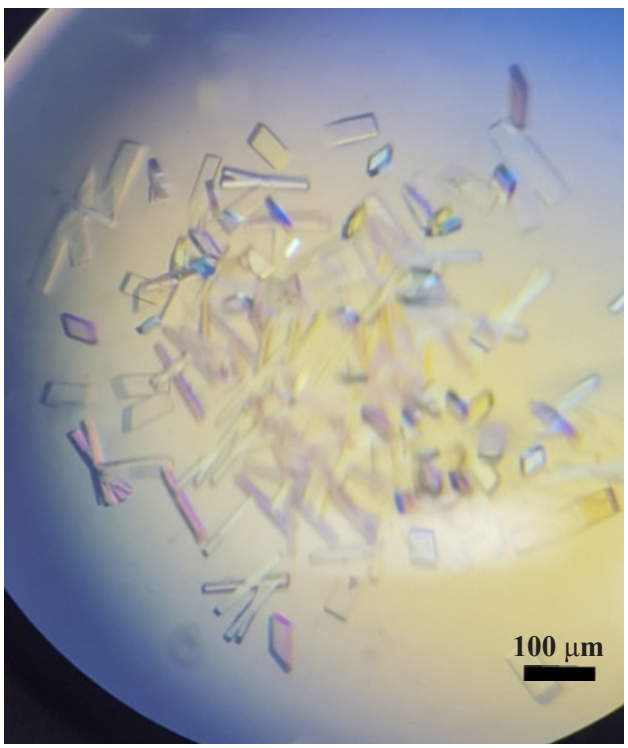

FIGURE 2 | Crystals of the MexT RD protein. The approximate dimension of the crystals is 100, 50, 30 μm. The scale bar represents 100 μm as indicated.

protein was expressed as the inclusion body, which did not allow further structural works. Thus, the RD (residues 96-305) was expressed in the pPROEX-HTA vector system (Invitrogen, USA). Multiple chromatographic steps were employed to purify the recombinant protein containing the hexahistidine tag at the N-terminus with a TEV protease cleavage site. Ni-NTA affinity chromatography was used for the initial purification from the

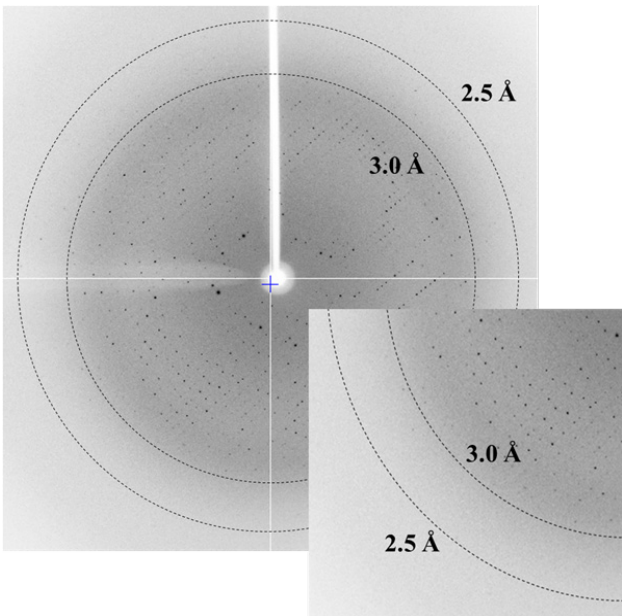

FIGURE 3 | A representative diffraction image. The resolution circles for 2.5 Å and 3.0 Å are shown in dotted lines. A rectangular area is enlarged in the right atom corner.

soluble lysate of the cultured *E. coli* cells, and the pooled protein was further purified using anion-exchange chromatography. The hexahistidine tag was removed by treating the recombinant TEV protease, and cleared the TEV protease and the cleaved tag by passing Talon resin. The final protein sample was concentrated to 23 mg/ml, which was measured by Bradford assay, with a high purity of >98% on SDS-PAGE (Figure 1). The protein band apparently appeared in a molecular weight of 23 kDa on the SDS polyacrylamide gel, which is well matched to the theoretical value (23.0 kDa).

We obtained the crystals under only one condition from about 500 premade conditions, by using an automated protein crystallization screening device. The crystallization conditions were optimized using 15 well plate at 14ºC with the hanging-drop diffusion method. The final reservoir solution contains 0.5 M ammonium sulfate, 1.0 M sodium citrate tribasic dehydrate (pH 5.6), 0.1 M lithium sulfate, and 2 mM EDTA, resulting in thick plate-shaped crystals (Figure 2). The MexT RD protein crystals were flash-cooled in liquid nitrogen after being briefly soaked in cryo-protection solution by adding 30% (v/v) glycerol to the reservoir solution. An undulator X-ray beam (beamline 7A in Pohang Accelerator Laboratory, Pohang, Republic of Korea) was utilized at a wavelength of 0.97934 Å to collect the diffraction dataset. The detector distance was maintained at 298.55 mm to collect the diffraction data. The dataset with 99.5% completeness and 2.5 Å resolution was finally collected (Figure 3). The crystal lattice belonged to the primitive orthogonal space group, and analysis of diffraction along the *h, k* and *l* axes further revealed a space group of $P2_12_12_1$ with unit cell parameters of *a*

= 65.7, *b* = 108.5, and *c* = 109.1 Å.

Crystal content analysis by Phenix program suite (Zwart et al., 2008) suggested that 3 or 4 molecules are contained in the asymmetric unit. Given a homodimer is the common oligomeric form of the RDs of the LysR-type regulators (Jo et al., 2015), it is more likely that 4 molecules (or 2 dimers) are in the asymmetric unit. There were extensive trials using the RD structures of many other LysR-type transcription regulators including DntR from *Burkholderia* sp. strain DNT, the closest homologue protein (PDB ID code: 2Y7R) with sequence identity 29% (Devesse et al., 2011). Unfortunately, the molecular replacement was not successful. We are now under growing Se-Met substituted crystals for phasing.

METHODS

Construction for the protein expression

The gene coding for the RD (residues 96-305) of MexT (NCBI reference sequence: AJ007825.1) was amplified from the genomic DNA from P. aeruginosa PAO1 by using PCR. Table 1 describes the primer sequences used for PCR. The PCR products were digested with restriction enzymes NcoI and XhoI, cloned into the two sites in pPROEX-HTA vector (Invitrogen, USA), resulting in pPROEX-HTA-MexT-RD that contains the hexahistidine tag at the N-terminus of the protein for purification and a TEV protease site for removing the tag (Table 1).

Protein expression and purification

Escherichia coli BL21 (DE3) cells were employed as the expression host by transforming the recombinant plasmid pPROEX-HTA-MexT-RD. The bacterial cells were cultured in 1.6 L LB medium supplemented with 100 μg/mL ampicillin at 37°C until OD_{600} reached 0.8. By adding 0.5 mM IPTG to the culture medium, induction of the MexT RD was triggered. Further culture at 30°C for 6 hours after induction, the cells were harvested by centrifugation at 1400xg for 10 min at 4°C. The cell pellet was resuspended with 50ml of lysis buffer containing 20 mM Tris (pH 8.5), 300 mM NaCl, 5% (v/v) glycerol, and 2 mM β-mercaptoethanol. The cells were disrupted by using sonicator, and centrifugation was conducted by at 20000xg for 30 min at 4°C to remove the cell debris.

TABLE 1 | MexT RD production information

	MexT RD
Source organism	*Pseudomonas aeruginosa* PAO1
DNA source	*Pseudomonas aeruginosa* PAO1 genomic DNA
Forward primer	GGAATCCATGGCGACCAGCACCGCGGTG
Reverse primer	GGCCTCGAGTTAGAGACTGTCCGGATCGCCG
Expression vector	pProEx-Hta
Expression host	*E. coli* BL21 (DE3)
Complete amino-acid sequence of the construct produced	RKTYYHHHHHHDYDIPTTENLYFQGAMATSTAV FRIGLSDDVEFGLLPPLLRRLRAEAPGIVLVVRRA NYLLMPNLLASGEISVGVSYTDELPANAKRKTV RRSKPKILRADSAPGQLTLDDYCARPHALVSFA GDLSGFVDEELEKFGRKRKVVLAVPQFNGLGTL LAGTDIIATVPDYAAQALIAAGGLRAEDPPFETRA FELSMAWRGAQDNDPAERWLRSRISMFIGDPD SL (Underlined residues are cleaved off by the TEV treatment)

Ni-NTA agarose resin (2 ml; Qiagen, Germany) was added to 50 ml of the cell lysate solution and rolled in a column for 40 min at 4°C. The resin was washed with 300 ml of a buffer containing 20 mM Tris (pH 8.5), 300 mM NaCl, 20 mM imidazole (pH 8.0), 5% (v/v) glycerol and 2 mM β-mercaptoethanol, and then the protein was subsequently eluted with 30 ml of a buffer containing 20 mM Tris (pH 8.5), 50 mM NaCl, 250 mM imidazole (pH 8.0), 5% (v/v) glycerol, and 2 mM β-mercaptoethanol. The fractions of the protein were pooled and was further purified with the anion exchange chromatographic column by applying a gradient from 0 mM to 1 M NaCl. The protein was eluted in a range of 200-250 mM NaCl, and was treated with a recombinant TEV protease for 6 hours at room temperature. The TEV protease and the cleaved hexahistidine tag was removed by passing through Talon resin (0.4 ml) two times. After concentration to 5 ml using a Vivaspin centrifugal concentrator (30 kDa molecular-weight cutoff; Millipore, USA), the resulting protein solution was further purified using a gel filtration chromatographic column (HiLoad 16/60 Superdex 200; GE Healthcare), which was pre-equilibrated with 20 mM Tris buffer (pH 8.5) containing 300 mM NaCl, 5% (v/v) glycerol and 2 mM β-mercaptoethanol. The pooled fractions were concentrated to 23 mg/ml using the same concentrator, and stored frozen at -80°C until use.

Crystallization

An automated crystal screening device MOSQUITO was employed for initial crystallization trials of the MexT RD protein at 14°C with sitting-drop vapour-diffusion method. Five matrix screening solutions (MCSG 1T, 2T, 3T, 4T, and Hampton Research Crystal Screen) commercially available were selected. The protein solution (0.2 μl, 23 mg/ml) was mixed with a reservoir solution (0.2 μl) and equilibrated against 60 μl of the reservoir solution in a 96-well crystallization plate. Tiny thick plate-shaped crystals appeared under the reservoir solution containing 05 M ammonium sulfate, 1.0 M sodium citrate tribasic dehydrate (pH 5.6), and 0.1 M lithium sulfate. The crystallization conditions were optimized with the hanging-drop

TABLE 2 | X-ray diffraction and cell content analysis

	MexT RD	
Data collection		
Beam line	PAL 7A	
Wavelength (Å)	0.97934	
Rotation range per image (°)	1	
Total rotation range (°)	360	
Exposure time per image (s)	1	
Space group	$P2_12_12_1$	
Cell dimensions		
a, b, c (Å)	65.7, 108.5, 109.1	
Resolution (Å)	50.0-2.50	
Total No. of reflections	27616	
No. of unique reflections	243	
R_{merge}	0.093 (0.386)	
High resolution shell CC1/2	0.531	
$I/\sigma I$	19.0 (3.6)	
Completeness (%)	99.5	
Redundancy	9.3 (5.9)	
No. of molecules in asymmetric unit	3	4
V_M (Å^3/Da)	2.84	2.11
Solvent contents (%)	0.552	0.402

* Values in parentheses are for the highest resolution shell.

diffusion method under a reservoir solution containing 0.5 M ammonium sulfate, 1.0 M sodium citrate tribasic dehydrate (pH 5.6), and 0.1 M lithium sulfate at 14℃. In the final optimization experiments, we obtained larger thick plate-shaped crystals suitable for data collection in 5-7 days (Figure 2) by mixing 1 μl of the protein solution (11.5 mg/ml) and 1 μl of the reservoir solution supplemented with 2 mM EDTA, and equilibration against 500 μl of the reservoir solution in a 15-well plate.

Data collection and processing

For data collection under cryogenic conditions, the crystals were transferred to 2 μl of cryo-protection buffer containing 0.35 M ammonium sulfate, 0.7 M sodium citrate tribasic dehydrate (pH 5.6), 0.07 M lithium sulfate, and 30% (v/v) glycerol. The crystals incubated in the cryo-protection buffer for 3 sec were flash-cooled in liquid nitrogen. The datasets were collected on ADSC quantum Q270 CCD detector in beamline 7A of Pohang Accelerator Laboratory, Republic of Korea, at a wavelength of 0.97934 Å. The program HKL-2000 was used to process, merge, and scale the diffraction datasets (Otwinowski and Minor, 1997). Table 2 describes the data-collection statistics.

CONFLICTS OF INTEREST

The authors declare that they have no conflict of interest.

ACKNOWLEDGEMENTS

This research was supported by Korea Institute of Planning and Evaluation for Technology in Food, Agriculture, Forestry (IPET) through Agriculture, Food and Rural Affairs Research Center Support Program, funded by Ministry of Agriculture, Food and Rural Affairs (MAFRA) (710012-03-1-HD120 to NCH). This work was also supported by grants from the National Research Foundation of Korea (NRF-2017R1A2B2003992 to NCH). We made use of beamlines 7A at Pohang Accelerator Laboratory (Pohang, Republic of Korea).

Original Submission: May 15, 2018
Revised Version Received: Jun 5, 2018
Accepted: Jun 6, 2018

REFERENCES

Devesse, L., Smirnova, I., Lonneborg, R., Kapp, U., Brzezinski, P., Leonard, G.A., and Dian, C. (2011). Crystal structures of DntR inducer binding domains in complex with salicylate offer insights into the activation of LysR-type transcriptional regulators. *Mol Microbiol* **81**, 354-367.

Fargier, E., Mac Aogain, M., Mooij, M.J., Woods, D.F., Morrissey, J.P., Dobson, A.D., Adams, C., and O'Gara, F. (2012). MexT functions as a redox-responsive regulator modulating disulfide stress resistance in Pseudomonas aeruginosa. *J Bacteriol* **194**, 3502-3511.

Jang, Y., Choi, G., Hong, S., Jo, I., Ahn, J., Choi, S.H., and Ha, N.C. (2018). A Novel Tetrameric Assembly Configuration in VV2_1132, a LysR-Type Transcriptional Regulator in Vibrio vulnificus. Mol Cells.

Jeong, H., Kim, J.S., Song, S., Shigematsu, H., Yokoyama, T., Hyun, J., and Ha, N.C. (2016). Pseudoatomic Structure of the Tripartite Multidrug Efflux Pump AcrAB-TolC Reveals the Intermeshing Cogwheel-like Interaction between AcrA and TolC. *Structure* **24**, 272-276.

Jo, I., Chung, I.Y., Bae, H.W., Kim, J.S., Song, S., Cho, Y.H., and Ha, N.C. (2015). Structural details of the OxyR peroxide-sensing mechanism. *Proc Natl Acad Sci U S A* **112**, 6443-6448.

Juarez, P., Broutin, I., Bordi, C., Plesiat, P., and Llanes, C. (2018). Constitutive activation of MexT by amino acid substitutions results in MexEF-OprN overproduction in clinical isolates of Pseudomonas aeruginosa. Antimicrob Agents Chemother.

Kim, J.S., Jeong, H., Song, S., Kim, H.Y., Lee, K., Hyun, J., and Ha, N.C. (2015). Structure of the tripartite multidrug efflux pump AcrAB-TolC suggests an alternative assembly mode. *Mol Cells* **38**, 180-186.

Kohler, T., Epp, S.F., Curty, L.K., and Pechere, J.C. (1999). Characterization of MexT, the regulator of the MexE-MexF-OprN multidrug efflux system of Pseudomonas aeruginosa. *J Bacteriol* **181**, 6300-6305.

Kohler, T., Michea-Hamzehpour, M., Henze, U., Gotoh, N., Curty, L.K., and Pechere, J.C. (1997). Characterization of MexE-MexF-OprN, a positively regulated multidrug efflux system of Pseudomonas aeruginosa. *Mol Microbiol* **23**, 345-354.

Li, X.Z., Plesiat, P., and Nikaido, H. (2015). The challenge of efflux-mediated antibiotic resistance in Gram-negative bacteria. *Clin Microbiol Rev* **28**, 337-418.

Otwinowski, Z., and Minor, W. (1997). Processing of X-ray diffraction data collected in oscillation mode. *Methods Enzymol* **276**, 307-326.

Song, S., Kim, J.S., Lee, K., and Ha, N.C. (2015). Molecular architecture of the bacterial tripartite multidrug efflux pump focusing on the adaptor bridging model. *J Microbiol* **53**, 355-364.

Tian, Z.X., Mac Aogain, M., O'Connor, H.F., Fargier, E., Mooij, M.J., Adams, C., Wang, Y.P., and O'Gara, F. (2009). MexT modulates virulence determinants in Pseudomonas aeruginosa independent of the MexEF-OprN efflux pump. *Microb Pathog* **47**, 237-241.

Zwart, P.H., Afonine, P.V., Grosse-Kunstleve, R.W., Hung, L.W., Ioerger, T.R., McCoy, A.J., McKee, E., Moriarty, N.W., Read, R.J., Sacchettini, J.C., Sauter, N.K., Storoni, L.C., Terwilliger, T.C., and Adams, P.D. (2008). Automated structure solution with the PHENIX suite. *Methods Mol Biol* **426**, 419-435.